Journal of the Korean Society of Oceanography
Vol. 35, No. 1, pp. 16—33, March 2000

The Vertical Fluxes of Particles and Radionuclides in the East Sea

DEOK-SOO MOON*, KEE-HYUN KIM AND IL NOH[1]
Department of Oceanography, Chungnam National University, Taejon 305-764, Korea
[1]Department of Environmental Engineering, Korea Maritime National University, Pusan 606-791, Korea

In order to measure the vertical fluxes of particles and reactive radionuclides such as thorium and polonium isotopes, Dunbar-type sediment traps were freely deployed at the Ulleung Basin and in warm and cold water masses around the polar front of the East Sea. We estimated the ratios of the catched (F) to the predicted ^{234}Th fluxes (P) using natural tracers pair ^{234}Th-^{238}U. The F/P ratios are decreased with increasing water depth. Whereas the concentrations of suspended particles are homogeneous in water column, the mass fluxes are also decreased with increasing water depth like the F/P ratios. These facts indicate that organic matters of settling particles are destructed within the euphotic layer due to decomposition. Whereas regenerations of sinking particles are negligible in the cold water mass, about 80% of them are regenerated in the warm water mass during falling of large particles. These downward mass fluxes are closely correlated with their primary productions in euphotic zone. The activities of ^{234}Th, ^{228}Th and ^{210}Po in the sinking material were increased with water depth. Because ^{234}Th steadily produced in the water column are cumulatively adsorbed on the surface of sinking particles, vertical ^{234}Th fluxes were observed to increase with water depth. Therefore, these sinking particles play important roles in transporting the particle reactive elements like thorium from surface to the deep sea. The scavenging processes including adsorption and settling reactions generate radio-disequilibrium between daughter and parent nuclides in water column. The activity ratios of ^{234}Th/^{238}U and ^{228}Th/^{228}Ra were observed to be < 1.0 in the surface water and approached to be equilibrium below the thermocline. The extent of the deficiency of daughter nuclides compared to the parents nuclide was highly correlated with the vertical particle flux. Because most of the ^{210}Po in the surface water are scavenged on a labile phase and are recycled at sub-surface depths (< 200 m), the ^{210}Po are always observed to be excess activities compared to ^{226}Ra in surface water.

INTRODUCTION

Particles in the ocean are theoretically classified into suspended and sinking materials according to the sampling method: the suspended materials are characterized by long residence time in water column due to negligible setting velocities (S≈0 m/y) and do not substantially contribute to the vertical particles flux in the ocean (Tsunogai *et al.*, 1994). Because most of particles in seawater exist in suspended phase (McCave, 1975), the suspended particles can be mainly collected by *in situ* filtration of seawater.

On the other hand, the sinking particles collected in the sediment traps are characterized by short residence time due to high settling velocities in water column (Bacon *et al.*, 1985; Cochran *et al.*, 1993; Huh *et al.*, 1993). The settling rates of sinking particles were estimated to be 6−10 m/day in the Santa Monica Basin, offshore California (Huh *et al.*, 1993) and 150 m/day in many studies about scavenging of radionuclides (Clegg and Whitfield, 1991; Nozaki *et al.*, 1987). Large particles, fecal materials and aggregates of suspended particles (marine snow) may play an important role in vertical mass transport (Bacon *et al.*, 1985; Clegg and Whitfield, 1993; Cochran *et al.*, 1993).

Only five to ten percentage of total thorium activities in seawater was found in suspended particles fractions in the open ocean. Studies on sinking particles and the vertical flux have not yet conducted in the East Sea. Direct observation of sinking particles using sediment trap is one of the best ways to study the vertical mass flux.

Studies on sediment trap show that vertical flux reflects the seasonality of productivity (Bacon *et al.*, 1985; Deuser *et al.*, 1981) because the vertical transport of material from water to sediment column is

*Present address: Chemical Oceanography Division, Korea Ocean Research and Development Institute, Ansan P.O. Box Seoul 425-600, Korea. dsmoon@kordi.re.kr

directly linked to surface primary production. Bruland *et al.* (1981) confirmed that the vertical fluxes and chemical composition of sinking materials agreed favorably with those deposited in bottom sediments. The vertical fluxes of radionuclides and metals measured using sediment traps have also been related to those of these materials estimated in the sediment column (Bacon *et al.*, 1985; Jickells *et al.*, 1984; Wei and Murray, 1992). Estimates of the nuclide fluxes measured by traps agree well with those predicted from the disequilibrium between the parents-daughter pair in water column (Bacon *et al.*, 1985; Huh *et al.*, 1993). Recently, some radioactive nuclide pairs, ^{228}Th-^{228}Ra, ^{210}Pb-^{226}Ra and ^{234}Th-^{238}U, have been used to study the settling mechanism such as aggregation and disaggregation of the suspended matter (Clegg and Whitfield, 1993; Cochran *et al.*, 1993; Huh and Beasley, 1987; Kaufman *et al.*, 1981). A radioactive disequilibrium is observed between a particle reactive daughter nuclides and their parent nuclides soluble in seawater, such as ^{234}Th-^{238}U, ^{230}Th-^{234}U, ^{210}Pb-^{226}Ra and ^{228}Th-^{228}Ra. Because these daughter nuclides are produced at exactly known rates by decay of their parent nuclides and rapidly scavenged onto particulate materials, the extent of disequilibria between parent and daughter nuclides could be used to estimate scavenging rates of the particle reactive elements by sinking particles in the ocean.

Thorium, one of the most particle reactive elements in seawater, has six radioactive isotopes in nature: Nonradiogenic ^{232}Th ($t_{1/2}$=1.4×10^{10} years) is fully carried into the ocean through continental weathering, whereas the other nuclides such as ^{230}Th ($t_{1/2}$=75,200 years), ^{228}Th ($t_{1/2}$=1.9 years), and ^{234}Th ($t_{1/2}$=24 days) are generated by the decay of their parent nuclides, ^{234}U, ^{228}Ra and ^{238}U in the seawater. Also, ^{210}Pb and ^{210}Po could be applied to study the fate of reactive elements introduced to the oceans (Bacon *et al.*, 1976; Chung and Finkel, 1988; Suzuki, 1994). ^{210}Pb ($t_{1/2}$=22.2 years) and ^{210}Po ($t_{1/2}$=138.4 days) are adequate to evaluate scavenging processes of particulate materials operating in the oceans considering their time scales. Because of their high chemical reactivity, these nuclides are used as tracers in evaluating elemental scavenging processes by particulate matter (Coale and Bruland, 1985; Huh and Beasley, 1987; Kaufman *et al.*, 1981; McKee *et al.*, 1984; Nozaki *et al.*, 1987; Nozaki and Yamada, 1987).

The aim of this study is to determine how particles and particle reactive radionuclides are transported from surface to deep sea and how these downward transport fluxes of particles in the water column are related to fluxes of the particle reactive radionuclides. To evaluate the particle dynamics during falling of particles, we have determined the ratios (F/P) of the catched (F) to predicted flux (P) using the ^{234}Th-^{238}U pair. This is done by carrying out radiochemical analysis of sinking particles collected in sediment traps and estimating the disequilibrium of parents and daughter nuclides in water column of the East Sea.

MATERIAL AND METHODS

Study area

Figure 1 shows stations where large volume of seawater was sampled using Niskin sampler and sediment traps were deployed. Station A2 was located at the southern Ulleung Basin, where water depth gradually increases northward from the Korea Strait. Seasonal upwellings are observed at the coastal region around A2 from April to October. Water temperatures in this station were observed to be 3—4°C lower than that of surrounding sea and the polar front region (Fig. 2). The other stations (A4, A11 and B10) were located in the polar front regions of the East Sea (Table 1). Station A4 was located in warm water mass and B10 in cold water mass. Station A11 was located in the middle of polar front. An array of three sediment traps were deployed in each station. A large volume of water were sampled with 30-liters Go-flow samplers teflon coated from the same depth where traps were deployed.

Sampling methods

Sediment trap

Sinking particulate matters were collected with Dunbar-type conical sediment traps (Fig. 3) that were designed and fabricated by the third author of this paper (Noh, 1988). These sediment traps are similar to Soutar-type traps that had used in an intercalibration experiment in the Santa Barbara Basin in 1979 (Dymond *et al.*, 1981). Following the intercalibration, the Soutar trap was chosen as the simplest, most reliable sediment trap that enables to collect a large amount of sinking particles. Its conical geometry is possible to preconcentrate the collected particles due to the funnelling effects, and this nonclosing trap is easy to handle and redeploy in the sea. Because it is made of gel-coated fiberglass, the weight of Dunbar-type trap is only about 10 kg. Using

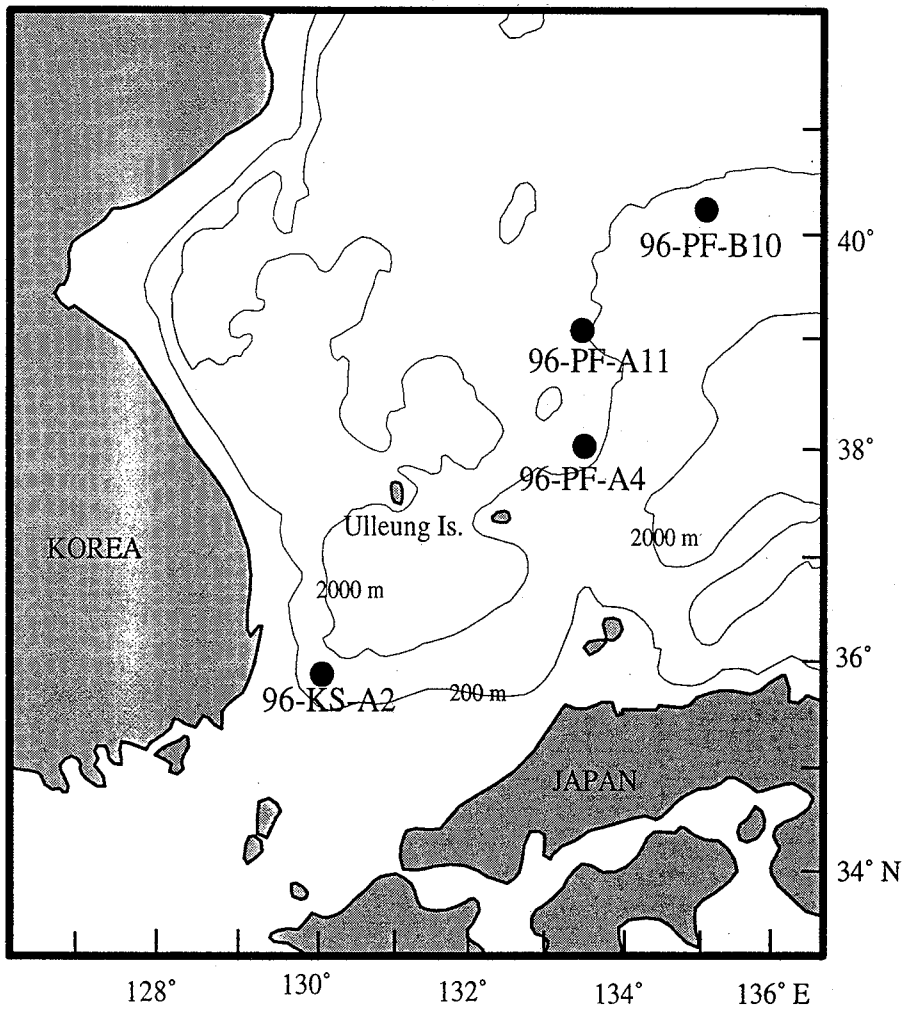

Fig. 1. Map showing the stations where large volume of seawater samples were collected and sediment traps were deployed. The stations were located in the Ulleung Basin and Polar Front area around 38°N.

the valved holes in the sides of the cone, most of the water overlying the collection chamber was easily drained off before hauling each trap on board, and with a simple manual block and trackle rig one can get a multiple trap array back aboard easily. Dunbar traps have a collecting cross section of 1,500 cm^2. The baffle used in the traps is an impregnated nylon honeycomb mesh with cells 1 cm wide by 2 cm deep. Laboratory flume studies indicate that a baffle with these dimensions prevents the penetration of turbulent eddies into the trapping chamber (Dymond *et al.*, 1981).

The traps were freely drifted as an array that had three sediment traps hung on the nylon line below a primary flotation sphere. A tracking buoy with radio beacon, radar reflector, flashing strobe and flag was fasten to this sphere. The broadcast of the radio beacon at VHF frequency could be tracked up to 10 miles away from the ship. Depending upon weather condition, the drift rate of the arrays and the tending duties of the ship times, the arrays were recovered after 24–36 hours. The sediment trap was set up close to the base of the mixed layer, 50 m depth to collect sinking material; the two additional traps within the thermocline at 100 m depth and below the thermocline at 200 m depth. The traps were poisoned with a brine solution to preserved the sinking materials. Immediately upon the recovery of the traps, large zooplanktons such as amphipoda and copepoda that were observed in the collection chamber were hand-picked using tweezers, which may swim into the trap and contribute error to the flux estimation. Each sample was wet split using a four-way splitter. The particulates were filtered by preweighted membrane filter (pore size=0.45 μm, 47 mm) and rinsed with deionized water to remove salt. The seawater drained from the sediment trap was also passed through membrane filter (pore size=0.45 μm, 142 mm). The filtrates were frozen and stored in freezer until analysis.

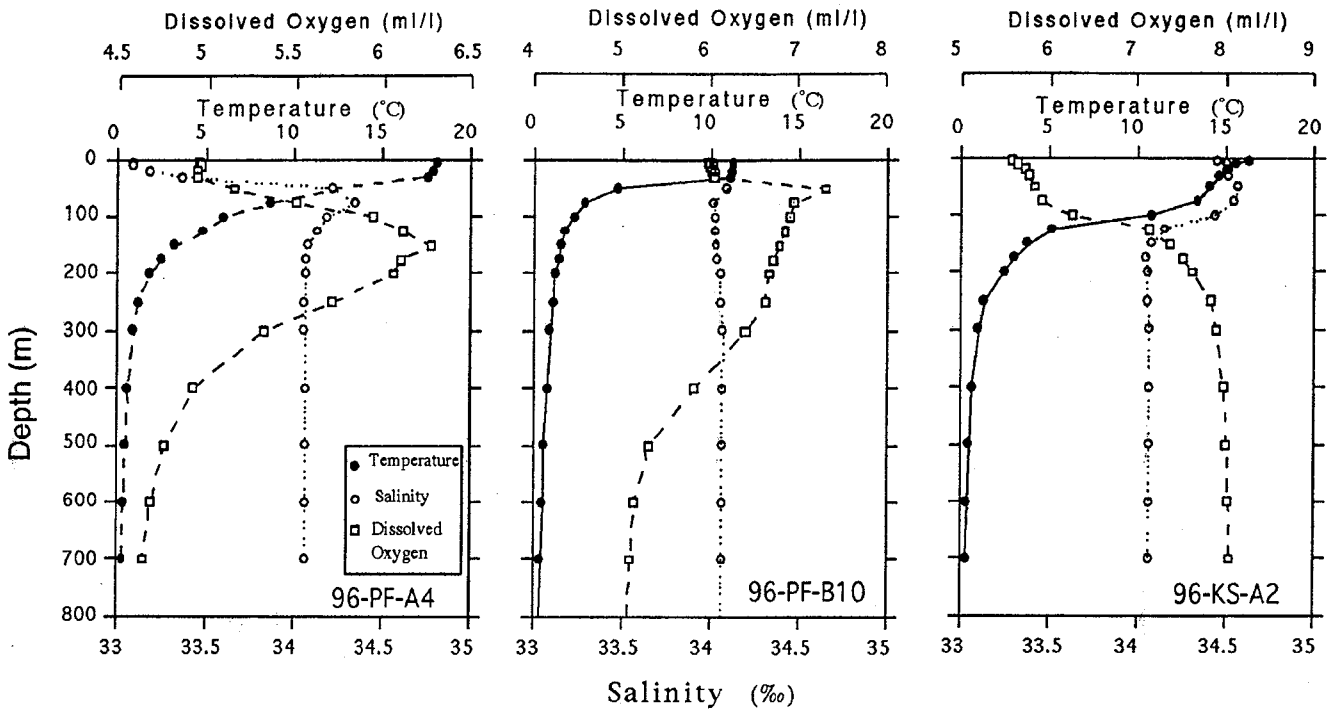

Fig. 2. The vertical profiles of salinity, temperature and dissolved oxygen in stations 96-PF-A4, 96-PF-B10 and 96-KS-A2, where, PF and KS represent the Polar Front and the Korea Strait. A2 station is located in the Southern Ulleung Basin, A4 in warm water mass and B10 in cold water mass around the polar front.

Table 1. Location of stations deploying sediment traps and time elapsed from the deployment to recovery, showing the characteristics of each water masses

Station I.D.	Location		Water epth (m)	Date deployed (m-d-y)	Date recovered (m-d-y)	Elapsed time (days)	Water masses
	Latitude (N)	Longitude (E)					
96-PF-A4	38°00.05'	133°40.11'	770	11-5-96	11-7-96	1.71	Warm water mass : Polar front
96-PF-B10	40°20.06'	135°00.11'	1400	11-9-96	11-14-96	4.34	Cold water mass : Polar front
96-KS-A2	35°46.54'	130°09.86'	1139	5-27-96	5-28-96	1.03	Tsushima Warm Current : Ulleung Basin

Analytical methods

Suspended particles were collected using large volume Niskin samplers and sinking particles using sediment traps at three sampling sites of the East Sea during cruises of R/V "TamYang" of KIOS (Korea Inter-University Institute of Ocean Sciences) in May and November 1996. After recovery, the seawater samples were treated on board according to the procedure referred in Figure 4. The procedures for determining thorium and polonium in seawater are based on methods developed by Anderson and Fleer (1982) and Harada and Tsunogai (1985). The β-activities of ^{234}Pa in radioactive equilibrium with ^{234}Th were counted with low background alpha/beta counter (Tennelec; LB5100), the α-activities of ^{228}Th and ^{232}Th were measured with silicon surface barrier detector, and the chemical yield of thorium was calculated from that of ^{229}Th. For the data of the short-lived ^{228}Th and ^{234}Th, the decay corrections for and after the trap deployment were made using the formula of Spencer *et al.* (1981).

RESULTS

Dry weights and Th and Po activities of sinking particles are listed in Table 2. Table 3 shows fluxes of particle mass and radionuclides. These fluxes are similar to the values estimated in the Santa Barbara Basin sediment by Moore *et al.* (1981). The mass fluxes were calculated based on the trap deploy time, cross area of sediment trap and dry weight of trapped materials. The vertical fluxes (F) of radionuclides

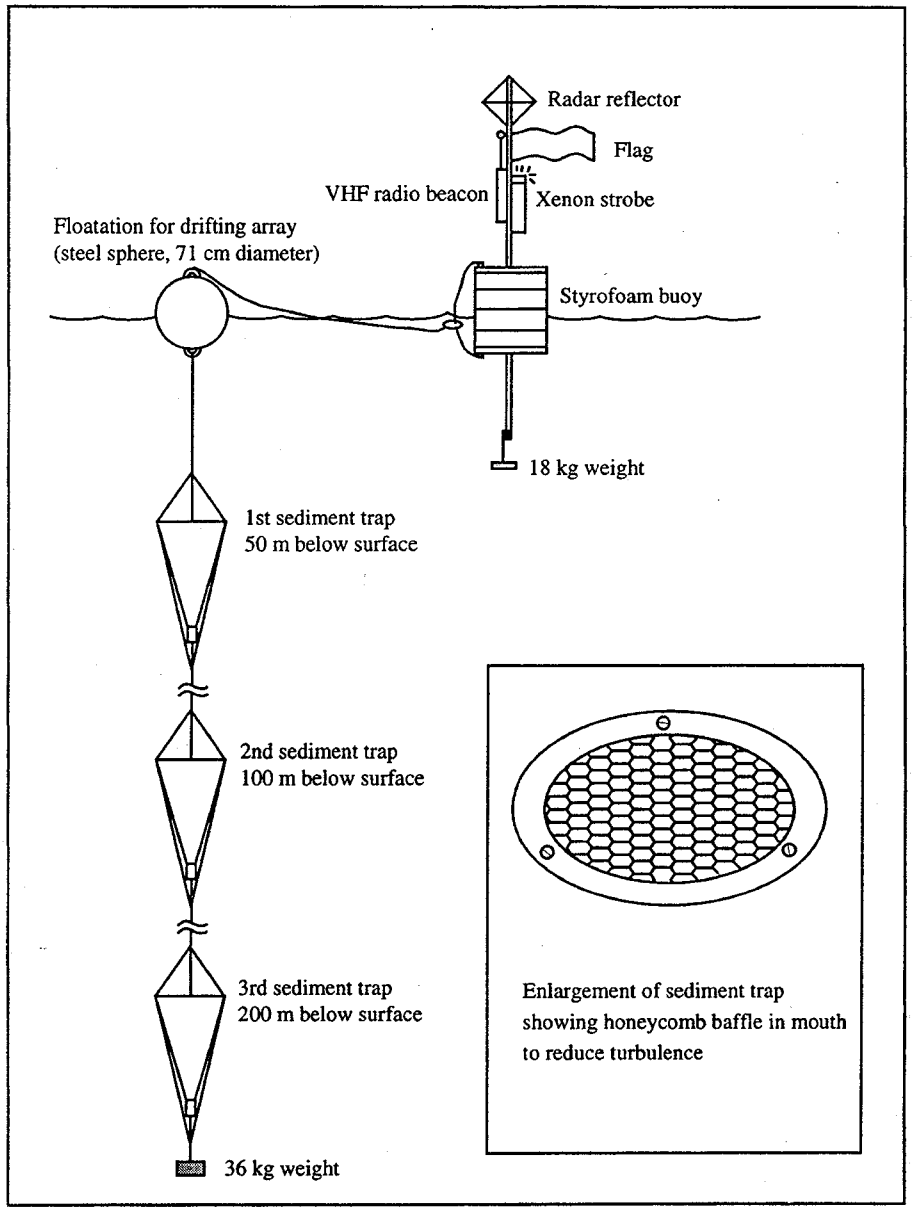

Fig. 3. A schematic diagram showing the floating sediment trap drift array used for sinking particle collections in this study.

were calculated by multiplying the mass flux (M) and specific activities (A) of radionuclides (F=M×A). ^{232}Th contents in sinking particles were the highest in Station A2 where terrigenous material dominates.

F/P ratios were estimated in water column of the East Sea, based on the catched flux (F) and the predicted flux (P) of ^{234}Th (Table 4). The predicted ^{234}fluxes were calculated from the deficiency between *in situ* production of ^{234}Th ($P_{.234Th}$) from parents nuclides (^{238}U) and standing stock (C) of ^{234}Th in water column ($P=P_{.234Th}-\lambda\times C$). The production rates were estimated by multiplying the concentration of the parent nuclide ^{238}U by the decay constant of the daughter isotope at water depths, 50 m, 100 m and 200 m ($P_{.234Th}=^{238}U\times\lambda^{234}$)

DISCUSSION

F/P ratio of ^{234}Th

It was not possible to exactly know the absolute collection efficiency of sediment trap in the ocean, because of the hydrodynamic conditions such as turbulent flow and trap design (Baker *et al.*, 1988; Butman *et al.*, 1986). In the case of the mooring trap deployment, trapping efficiency is inversely correlated with Reynold number, R_t, and current speed, whereas the mean mass flux collected by the free drifting trap was relatively uniform over several order of current speeds (Baker *et al.*, 1988). Therefore, we preferred free drifting deployment of the Dunbar type sediment

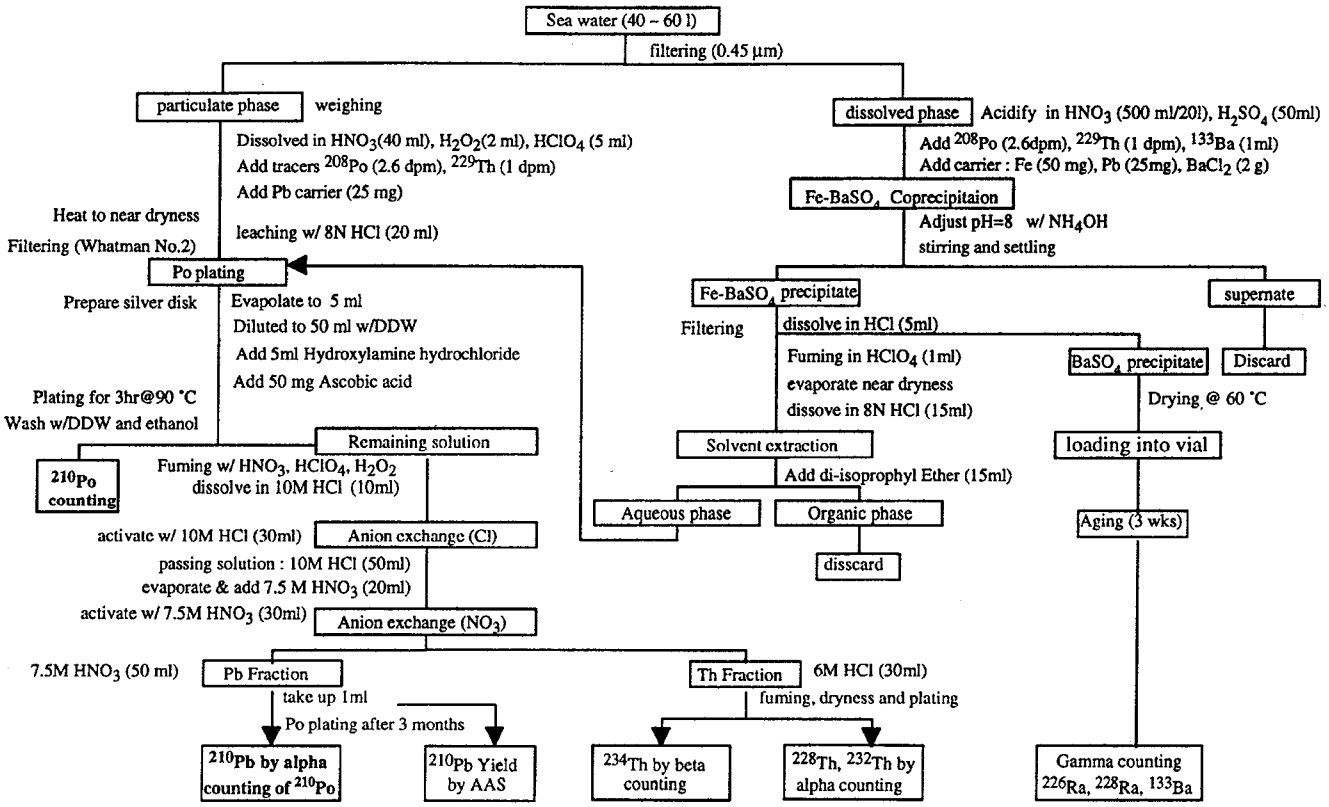

Fig. 4. A schematic illustration of simultaneous analytical procedures for radionuclides in dissolve state, suspended and sinking particles of the seawater.

Table 2. The dry weights of sinking particles and specific activities of Th and Po isotopes in sinking particles collected in sediment trap.

Sample I.D.	Depth (m)	Weight of trapped material (mg)	Radionuclides activity (dpm/g)			
			^{234}Th	^{228}Th	^{232}Th	^{210}Po
96-PF-A4	50	475.4	1063.8±82.5	12.67±0.70	5.66±0.44	88.50±5.31
	100	329.0	1455.6±121.4	16.57±0.71	6.92±0.41	150.04±12.19
	200	63.8	3968.7±183.0	69.60±2.89	21.58±1.37	814.87±78.92
96-PF-B10	50	370.0	1421.5±114.6	32.29±1.98	26.90±1.90	157.66±10.40
	100	149.4	5892.3±532.2	65.00±5.07	7.26±1.14	225.58±19.56
96-KS-A2	50	192.3	1123.0±34.8	2.06±0.13	0.81±0.08	42.51±2.94
	150	26.6	4627.0±155.0	4.84±0.48	2.09±0.31	138.40±13.67

traps, which were the simplest, most reliable for the collection of sinking particles (Gardner, 1980).

If we could exactly estimate the geochemical budgets of radionuclides existed in seawater, it is possible to use such radionuclides as tracers to evaluate the dynamics of particles in the ocean (Brewer *et al.*, 1980; Knauer *et al.*, 1979). The best candidate for this purpose is ^{234}Th, which is produced at exactly known rate by radio-decay of conservative ^{238}U dissolved in seawater. ^{234}Th produced from its parent nuclide is rapidly adsorbed on surface of settling particles and removed in the surface water as sinking particles. Therefore, residence time of ^{234}Th in water column was observed to be a few days (Anderson *et al.*, 1983a).

Calculation of the F/P ratio is based on the simple assumption that the theoretical particle flux (P) of ^{234}Th should be equal to the vertical particulate flux (F) catched using the sediment trap deployed in water column (F/P=(M−H)/P). This assumption is correct

Table 3. Fluxes of sinking particles and radionuclides measured by sediment traps in the East Sea. Fluxes of radionuclide, Th isotopes and Po, were calculated from fluxes of particles observed in sediment traps and their specific acitvies.

Station I.D.	Depth (m)	Mass flux (mg/m^2/d)	Corrected radionuclides flux (dpm/m^{2}d)			
			^{234}Th	^{228}Th	^{232}Th	^{210}Po
96-PF-A4	0—50	1729.1	1839.5	17.09	7.64	119.38
	0—100	1196.6	1741.8	33.12	13.83	299.85
	0—200	232.1	920.9	78.48	24.34	918.82
96-PF-B10	0—50	535.7	761.6	32.30	26.91	157.71
	0—100	216.3	1274.6	26.31	2.94	91.31
96-KS-A2	0—50	1388.4	1559.1	2.10	0.82	43.42
	0—150	192.1	888.9	4.17	1.79	119.24

Table 4. F/P represents the ratios of the measured flux (F) to the predicted one of ^{234}Th (P). F means ^{234}Th fluxes collected in sediment trap and P calculated from ^{238}U and ^{234}Th concentration in water column. Uranium concentrations in seawater were calculated from the relation with salinity (Ku et al., 1977).

Station I.D.	Depth (m)	Concentration ^{238}U ($\times 10^5$ dpm/m^2)	Production rate of ^{234}Th (dpm/m^2/d)	Standing stock of ^{234}Th in water (dpm/m^2/d)	Predicted ^{234}Th Flux (dpm/m^2/d)	Measured ^{234}Th Flux (dpm/m^2/d)	F/P ratio (%)
96-PF-A4	0—50	1.197	3440	2005	1435	1839	128.2
	0—100	2.382	6848	3939	2909	1742	59.9
	0—200	4.786	13763	9288	4475	921	20.6
96-PF-B10	0—50	1.205	3464	2042	1422	762	53.6
	0—100	2.409	6928	4543	2385	1275	53.4
96-KS-A2	0—50	1.222	3512	2365	1147	1559	135.9
	0—150	3.639	10464	6480	3984	889	22.3

only if there is no horizontal transport (H) by which ^{234}Th could be added to, or removed from, the water column. We could ignore the horizontal transports (H=0) because the floating sediment trap used in this study is drifting with water mass, then the vertical flux (F) is equal to the catched flux (M). Under steady state, the theoretical flux (P) can be calculated from the simple relationship; $P=P_{\cdot 234Th}-\lambda C$, where $P_{\cdot 234Th}$ and C represent, respectively, the production rate from the parent nuclides and the standing stock of ^{234}Th within the interested layer in water column. As for short lived ^{234}Th, the decay term becomes important, and one must know the distribution of ^{234}Th to calculate its theoretical scavenging flux (P).

The F/P ratios of traps in each layers are given in Table 3—4. The F/P ratios were estimated to be in the range of 130%—20%, higher in surface seawater and gradually decreased with increasing water depth, especially under thermocline (Table 4, Fig. 5). This trend may be explained by destruction of organic particles sinking through water column. Sinking rates of particles decrease in thermocline depth due to the density gradient of seawater, while their residence time increases. The particles can readily be destroyed by the degradation process of bacteria during sinking process across thermocline because the compositions of sinking particles mainly consist of organic matters (Broecker and Peng, 1982). We could find evidences for the regeneration in the profiles of particles mass flux (Fig. 6) and the profiles of dissolved and particulate ^{234}Th across thermocline in water column (Fig. 9). The vertical transport amounts of sinking material decreased linearly with increasing water depth, indicating dissolution of organic particles during falling. The ^{234}Th profiles of the dissolved and particulate phase have also shown "mirror images" each other, implying transformation of particulate ^{234}Th into dissolved phase (Fig. 9).

The F/P ratios in surface mixed layer (50 m) were estimated to be 130 percent in warm water mass (96-PF-A4 and 96-KS-A2). It is considered that these overestimated values were originated from the uncertainty of tracer activity, ^{234}Th, ($\approx$10%) and the high concentration of particles existed in surface seawater, which give the particle reactive element like ^{234}Th the more binding sites for scavenging. However, the

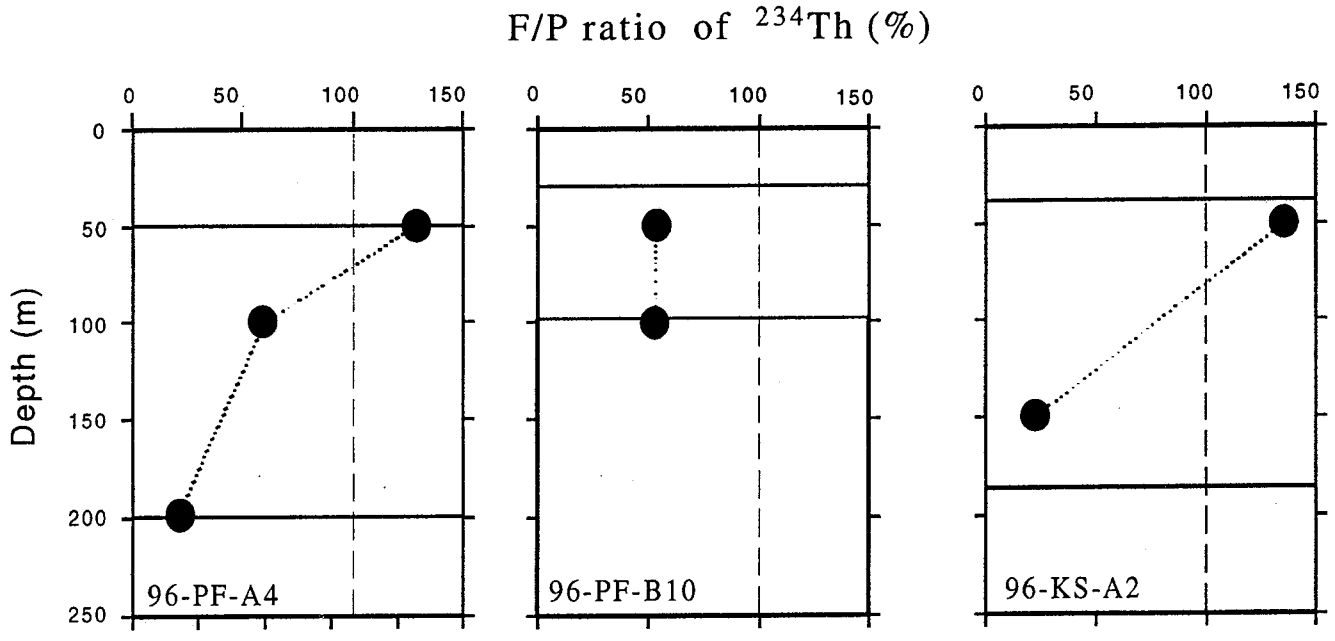

Fig. 5. The F/P ratios of the measured flux (F) to predicted flux (P) were estimated using ^{234}Th-^{238}U disequilibrium and ^{234}Th flux in seawater. The predicted fluxes were calculated from the equations as follows; $P=P_{234Th}-\lambda C$, where P_{234Th} represents the production of ^{234}Th from the parent nuclides, ^{238}U, and C indicate the standing stock of ^{234}Th in water column. The measured fluxes represent the directly observed fluxed using sediment trap.

F/P ratios in cold water mass (96-PF-B10) were estimated to be 50 percent at all depth and showed constant ratios with water depth unlike the ratios in warm water mass. This trend is origniated from low primary production in surface water of the cold water mass (87 mgC/m^2/day; KIOS, 1996), which reduces not only concentration of particles and downward flux of sinking particles but also the organic contents in particles (Fig. 7). Therefore, the constant F/P ratio at depth in station B10 was considered to reflect the reduction of organic particles regeneration.

Suspended and sinking material

Figure 6 shows the vertical mass flux of sinking materials and the concentration of suspended materials measured at the water depths. Fine suspended materials have characteristics such as relatively high concentrations and long residence time due to negligible setting velocities (McCave, 1975), and account for most of particles existing in seawater. The concentrations of the suspended materials were observed to be in the range of 0.31−0.47 mg/l and evenly distributed in the warm and cold water masses of the East Sea (96-PF-A4 and 96-PF-B10). Also, the concentration profiles of the suspended materials were vertically constant in water column, suggesting that the suspended particles play a minor role in transporting mass to deep sea. However, the particles concentrations in station A2 were measured to be 10.35 mg/l (May 1996) in surface water, showing higher concentrations than those at any other stations because the station A2 is located in coastal area where there are large amount of terrigenous materials from the land.

The vertical fluxes of sinking materials in warm water mass are rapidly decreased from 1730 to 232 mg/m^2/d with increasing water depth (96-PF-A4), and, in the cold water mass, from 536 to 216 mg/m^2/d (96-PF-B10). It was reported that the total mass fluxes varied from 60 to 20 mg/m^2/d in the Sargasso Sea (Deuser, 1981), from 770 to 410 mg/m^2/d in the North Atlantic Bloom Experiment (Buesseler *et al.*, 1992) and from 940 to 240 mg/m^2/d in the Santa Monica Basin with some seasonal variation (Huh *et al.*, 1993). Although the East Sea shows characteristics of the hemipelagic sea, the mass fluxes at this area were estimated to be relatively higher than those in Santa Monica Basin.

The vertical fluxes of materials from the surface mixed layers of warm water mass were observed to be 3−5 times higher than those in cold water mass, which may be originated from the difference in primary production in the two water masses. The daily

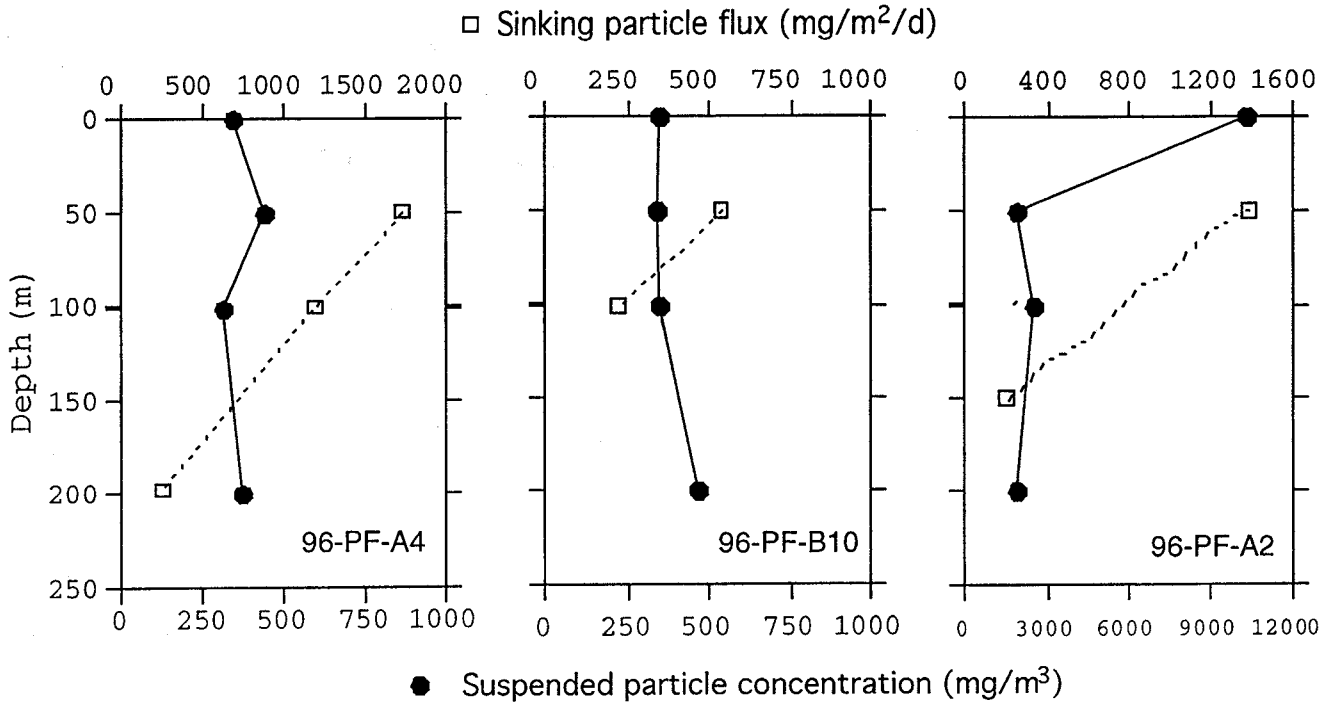

Fig. 6. Concentration of suspended particles (boxes) and the mass fluxes (circles) in water column of the East Sea. The suspended particle were collected by filtration of seawater and the mass fluxes (circles) using sediment traps.

primary productivity was measured to be 300 mgC/m²/d in the warm water mass (A4) and 87 mgC/m²/d in the cold water mass (KIOS, 1996). The productivity was observed to be about 3 times higher in warm water than in cold water mass as in the case of the mass flux.

Figure 7 shows concentration profiles of particulate organic carbon (POC) in warm and cold water masses. POC concentrations in both warm and cold water columns decrease exponentially above thermocline, while they reach to a uniformly low level in the deep sea. The euphotic zone is characterized by high and variable POC concentration due to primary production. Below the euphotic zone, because organic matter is oxidized faster than it is produced, so, POC concentrations are decreased with the increasing water depth as shown in Fig. 7. Thus, most of the sinking POC appears to be decomposed above thermocline. However, the decrease of POC concentrations in cold water mass (B9) was observed to be insignificant compared to warm water mass (B9).

Sediment trap data suggest that there is positive correlation between the flux of particulate materials and the primary production. Deuser and Ross (1980) and Deuser *et al.* (1981) observed that the particle flux even at great depth was closely correlated with the rate of surface primary production predicted from the historical data. Suess (1980) summarized the results of sediment trap deployments in the world's oceans and was able to describe the data well with a model that assumed the downward flux of organic carbon to be directly proportional to the rate of surface primary production. Although the concentrations of suspended material in the Korea Strait were observed to be higher compared to that in the Polar Fronts, the vertical mass flux in the Korea Strait is measured to be intermediate between the warm and cold water masses (Fig. 6). Because turbulence processes due to upwelling in this area may increase break-down of sinking particles, the mass flux during upwelling periods is not so great despite of high primary production (>700 mgC/m²/d; Shim and Park, 1986) and high suspended materials (Fig. 6). Organic contends in sinking materials were observed to be low in the surface of cold water mass due to the low primary productivity. Therefore, F/P ratios in the cold water mass were observed to be uniform because of weak re-generation of sinking organic material.

Fluxes of Th and Po isotopes

Radionuclides data of sinking particles, coupled with suspended and dissolved phases and material flux from euphotic zone to the deep sea could give us

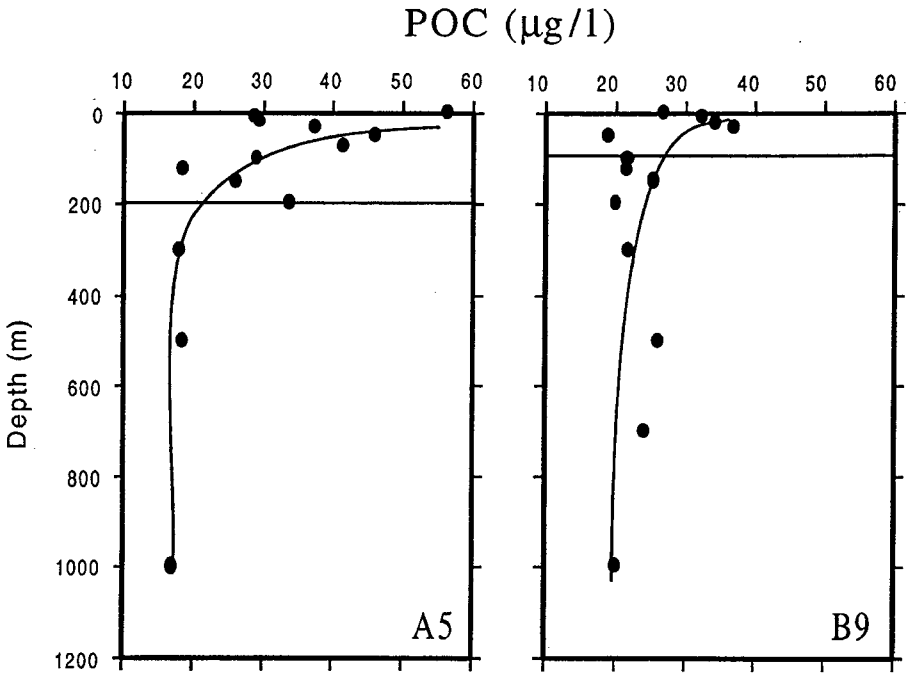

Fig. 7. The vertical profiles of POC (Particulate Organic Carbon) concentration in warm (A5) and cold water mass (B9). POC concentrations in warm water mass were decreased drastically with increasing water depth, while, in cold water mass, decreased slightly. These POC data are obtained from the KIOS report (1996).

some insight into geochemical processes of particles occurring within the East Sea. The vertical fluxes of sinking particles consisted of organic and inorganic material decrease with the increasing water depth due to dissolution of organic material within euphotic zone and thermocline. However, fluxes and specific activities of radionuclides in sinking particles (^{234}Th, ^{228}Th, ^{210}Po) increase with water depth (Fig. 7, 10 and 12). These facts indicate that Th atoms hydrated in seawater prefer to adsorb on the surface of inorganic particles, representing detrital particles to be the important carrier of vertical mass flux (Huh *et al.*, 1993). The vertical fluxes of these nuclides were calculated from the product of their specific activities and corresponding mass fluxes in the water column (Table 3). Thorium and polonium fluxes in the East Sea show a general increase with water depth because of scavenging of particle reactive nuclides. However, it is conceivable that the detailed association of Th isotopes with inorganic mineral phases is dictated by their sources and half-lives. ^{232}Th is the only non-radiogenic isotope in the family of thorium isotopes; essentially all of ^{232}Th is locked in the lattice structure of minerals. In contrast, nearly all ^{234}Th in sediment trap material is produced from ^{238}U decay in seawater and resides on particle surface as a result of scavenging. The behavior of ^{228}Th falls between these two extremes.

The scavenging processes produce the disequilibrium between daughter and parents nuclides. The activity ratios of ^{234}Th/^{238}U and ^{228}Th/^{228}Ra show less than 1.0 in surface water and then approached to equilibrium value below thermocline (Fig. 8 and Fig. 10). The deficiency of the daughter nuclides from their parents should be associated with the rate of removal by sinking particles.

^{234}Th

In the East Sea, the vertical fluxes of ^{234}Th were measured at three different stations. ^{234}Th fluxes (P) predicted by ^{234}Th depletion relative to its parent nuclide, ^{238}U, in water column were compared with the measured ^{234}Th fluxes (F) as F/P ratio (Fig. 5; Table 4). In euphotic zone of warm water mass, the predicted fluxes based on ^{234}Th standing stock agreed well with the measured ^{234}Th fluxes (96-PF-A4 and 96-KS-A2). However, in the cold water mass (96-PF-B10) with low primary production, the catched ^{234}Th fluxes were underestimated compared to the calculated ^{234}Th flux because settling particles in the cold water mass are not sufficient enough to carry Th isotopes from the surface to deep water.

The flux of ^{234}Th tends to increase with water depth from 1100−1435 to 4475 dpm/m^2/d in all three stations (Fig. 8 (a)), because ^{234}Th produced from parent nuclide that is conservatively distributed in seawater are cumulatively adsorbed on the surface of settling particles and finally removed from the surface water. The removals of ^{234}Th by the settling particles is found into the ^{234}Th depletion from the equilibrium

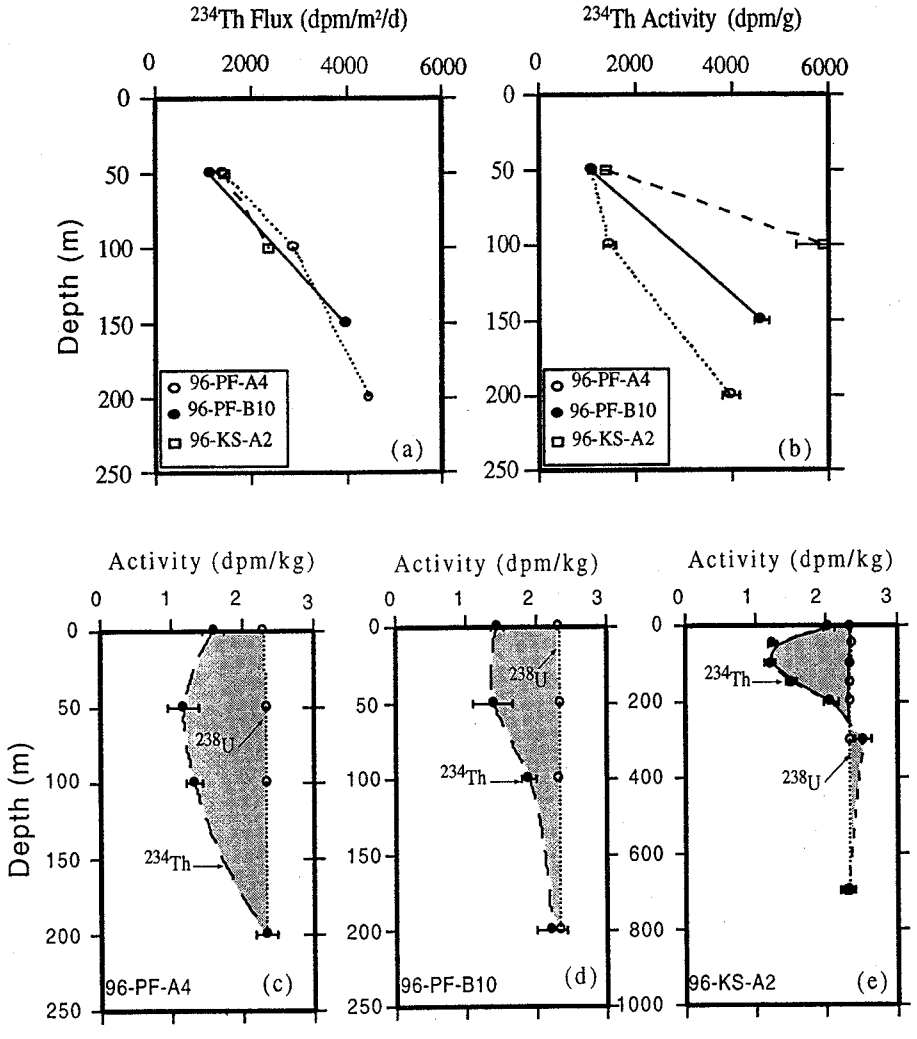

Fig. 8. The vertical profiles of ^{234}Th flux, specific activities of sinking particles and ^{234}Th and ^{238}U activities in dissolved and suspended parcels. (a) ^{234}Th fluxes measured by sediment traps deployed at three stations, (b) the ^{234}Th specific activities of the sinking particles and (c-e) ^{234}Th and ^{238}U activities of the dissolved phase and suspended particles at three stations. ^{238}U concentrations were calculated based on the relationship with salinity. Error bars indicate 1σ counting statistics.

with ^{238}U (Fig. 8 (c)-(e)) and the specific activity of settling particles increased with water depth (Fig. 8(b)), indicating the settling particles are important carriers that remove the reactive elements from the surface to the deep sea. Therefore, the extent of ^{234}Th deficiency in the surface water is closely correlated with the ^{234}Th flux.

Thorium-234 having 24.1 day half-life is produced almost uniformly in the water column by ^{238}U decay. However, most of the ^{234}Th scavenging occurs within the upper 200 m of water column (Moore *et al.*, 1981; Fig. 8 (c)-(e)). The disequilibrium between ^{234}Th and ^{238}U was measured to be 0.7−0.6 in surface waters, while $^{234}Th/^{238}U$ activity ratios approached to 1.0 below thermocline (Fig. 8). Also, in station 96-KS-A2, ^{234}Th deficiency was observed down to 300 m water depth, deeper than in polar front. $^{234}Th/^{238}U$ activity ratios were observed to be 0.64 in the surface layer of the coastal sea (96-KS-A2), 0.68 in 96-PF-B10 and 0.59 in 96-PF-A4 of polar front in the East Sea, indicating that 41% in 96-PF-A4, 36% in 96-KS-A2 and 32% in 96-PF-B10 of the ^{234}Th generated within the upper 150 m is removed by particle scavenging. The extents of ^{234}Th depletion within upper 150 meters were related to the degree of particles flux in the surface water, in the order of the amount of materials trapped at 50 m depth (96-PF-A4 > 96-KS-A2 > 96-PF-B10). It is indicated that settling particles are the practical carrier of reactive elements from the surface to deep water (Fig. 8 (c)-(e)).

We found a trend of increasing activities of the settling particles with water depth (Fig. 8 (b)), whereas the total mass of the sinking particles decreased with water depth due to the degradation of organic materials. The ^{234}Th specific activities in the sinking particles trapped at 50 m water depth are similarly observed in all three stations. Especially, the increase of ^{234}Th activity in settling particles is observed to be the greatest in the cold water mass (96-PF-B10) among three stations (Fig. 8 (b)). It implies that most

of thorium scavenging is controlled by the inorganic materials.

^{228}Th

Most of ^{228}Th are produced through ^{228}Ra decay in the upper ocean. ^{228}Th produced in water column is adsorbed on the surface of sinking particles and removed from surface water to sediment like ^{234}Th. The concentrations of ^{228}Ra are variable depending on the distance from the continental margin. ^{228}Ra is predominantly supplied to seawater from pore water after produced from ^{232}Th radiodecay in sediments, and through desorption from suspended particles in the estuarine mixing zone. Since Ra is not actively scavenged by particles, the ^{228}Ra derived from coastal and shelf sediments spreads over the surface ocean by lateral mixing, while undergoes radiodecay. Consequently, ^{228}Ra concentrations were gradually decreased with increasing distance from the shelf region toward polar front (Table 5; Fig. 10). ^{228}Ra concentrations in surface ocean of the East Sea were measured to be 332.4 dpm/10^3 kg in the Korea Strait (96-KS-A2), 246 dpm/10^3 kg in the warm water mass (96-PF-A4), 120 dpm/10^3 kg in the polar front mixing zone and 80 dpm/10^3 kg in the cold water mass (96-PF-B10), displaying north-eastward decrease from the Korea Strait (Fig. 11). A large amount of terrigenous sediments are deposited on the continental shelves around the Korea Strait, where ^{228}Ra in sediment is supplied to the overlying water column. This ^{228}Ra was advected to the polar front by currents and radio-decayed during its transport. Therefore, ^{228}Ra in surface water decreases horizontally toward polar front (Fig. 10).

We measured the ^{228}Th flux at the upper 50 m, 100 m and 200 m depth in three stations of the East Sea (Fig. 10 (a); Table 5). Generally, the ^{228}Th flux increased with water depth except a station in cold water mass (96-PF-B10). At the southern East Sea (A2), ^{228}Th fluxes were estimated to be 2.1 at 50 m and 4.2 dpm/m^2/d at 150 m. In the warm water mass (A4), ^{228}Th fluxes were enhanced from 17 dpm/m^2/d at 50 m to 79 dpm/m^2/d at 200 m. On the contrary, ^{228}Th fluxes at the cold water mass (96-PF-B10) were decreased from 32 dpm/m^2 d at 50 m to 26 dpm/m^2/d at 100 m. Because ^{228}Th in seawater is cumulatively adsorbed on the surface of sinking materials, its vertical flux increase with water depth. ^{228}Th fluxes in GEOSECS stations closest to Bermuda (Li *et al*, 1980) and the Saggasso Sea were measured to be 0.68-3.1 dpm/m^2/d (Bacon *et al*, 1985). ^{228}Th fluxes in the East Sea were estimated to be in the range of 2.1−32 dpm/m^2/d at 50 m, an order greater than that in the above pelagic oceans.

Unlike uniformly distributed ^{234}Th flux, ^{228}Th fluxes were observed to increase with distance from the Korea Strait because ^{228}Ra diffused out of the coastal sediment continuously produces ^{228}Th during their northward transport. Therefore, the increase of ^{228}Th flux may be generated from the scavenging during its transport. These facts are supported by the data that the ^{228}Th activities of the sinking material were increased in proportion to the distance from the ^{228}Ra source (Fig. 10 (b)).

Using ^{228}Th/^{228}Ra disequilibrium in seawater like the case of ^{234}Th/^{238}U, we could predict ^{228}Th flux removed from surface water (Fig. 10 (c)-(e)). The

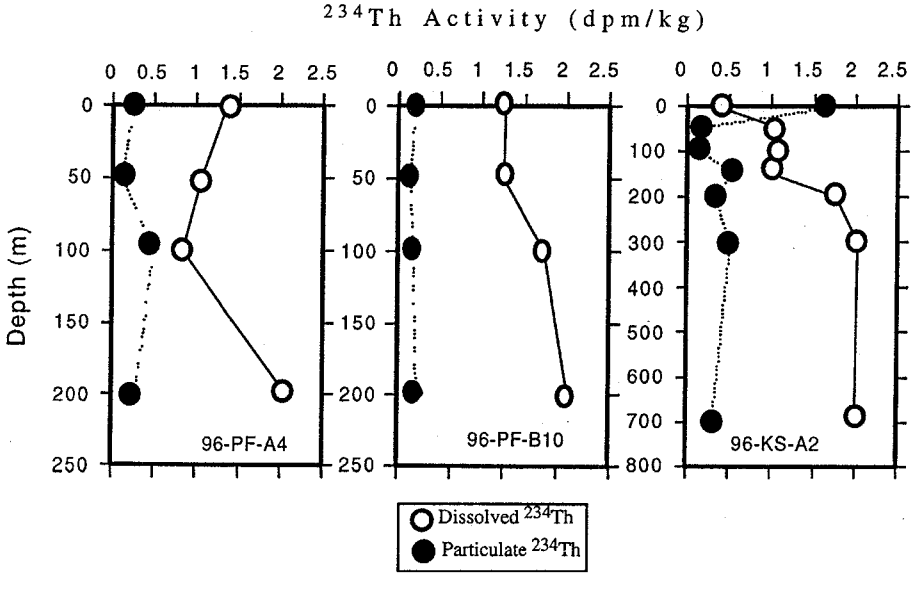

Fig. 9. The activity profiles of ^{234}Th existing in the dissolved and particulate phases at three stations. Open and closed circles represent the dissolved and particulate ^{234}Th activities, respectively.

Table 5. The F/P ratios were calculated by ^{228}Th flux predicted from ^{228}Ra in water column and ^{228}Th flux measured in sediment trap

Station I.D.	Depth (m)	Concentration ^{228}Ra ($\times 10^4$ dpm/m^2)	Water column production rate (P) (dpm/m^2/d)	Standing Stock of ^{228}Th in water (dpm/m^2/d)	Predicted ^{228}Th Flux (dpm/m^2/d)	Measured ^{228}Th Flux (F) (dpm/m^2/d)	F/P ratio (%)
96-PF-A4	0—50	0.96	9.65	409	9.24	17.09	1.85
	0—100	1.52	15.22	809	14.41	33.12	2.30
	0—200	2.50	24.96	1732	23.23	78.48	3.38
96-PF-B10	0—50	0.35	3.48	707	2.77	32.30	11.66
	0—100	0.65	6.51	1256	5.26	26.31	5.00
96-KS-A2	0—50	1.07	10.69	408	10.28	2.10	0.20
	0—150	2.37	23.65	893	22.75	4.17	0.18

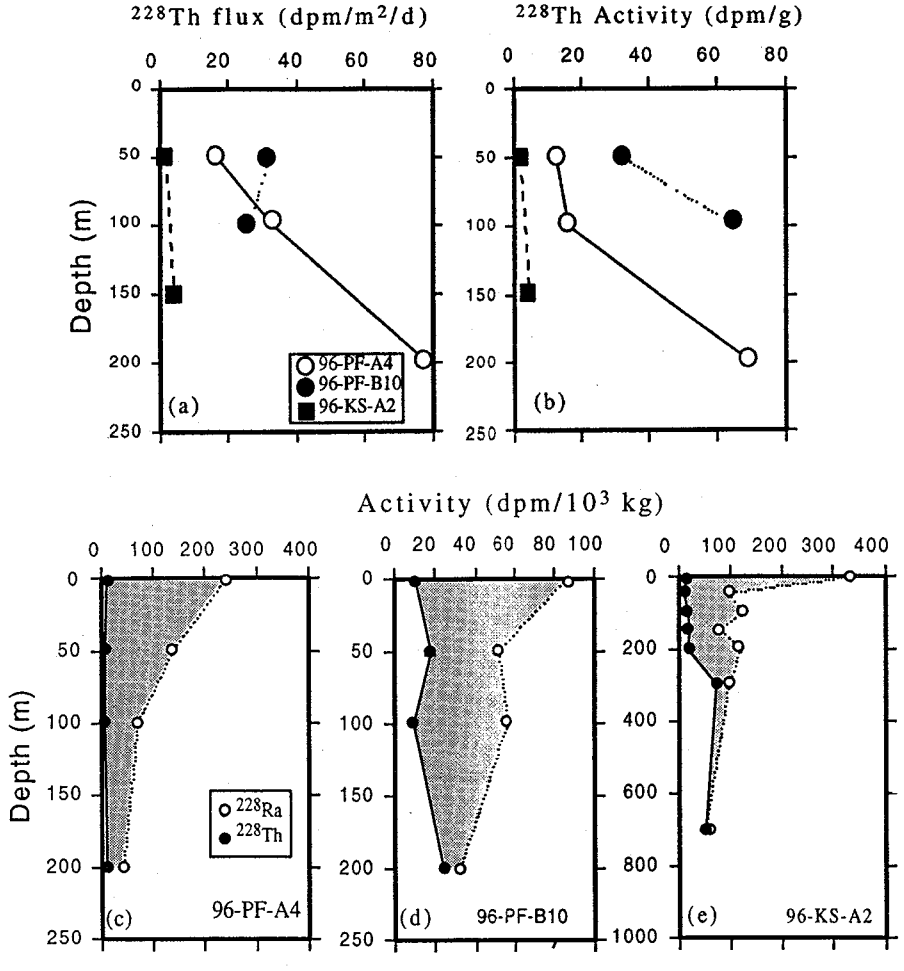

Fig. 10. ^{228}Th activities of dissolved phase, in suspended and sinking particles of water column. (a) ^{228}Th fluxes patterns according to water depth at three stations, (b) the ^{228}Th specific activities in the trapped material, and (c-e) ^{228}Th and ^{228}Ra profiles in water column.

measured ^{228}Th fluxes were observed to be 4 times higher at the polar front (96-PF-A4 and 96-PF-B10) compared to the predicted fluxes, whereas one-fifth times at the Ulleung Basin (96-KS-A2) (Table 5). Considering only ^{228}Th data in the dissolved, suspended and the sinking phases, it would be difficult to explain the difference between the predicted (P) and the catched fluxes (F). However, there are two additional effects that must be considered when predicting the ^{228}Th flux. Because ^{228}Ra diffused out from the shelf sediments was supplied into water column and have not resided enough time to generate ^{228}Th by radio-decay in the Korea Strait, the F/P ratio of ^{228}Th in station A2 were measured to be below 0.2. However, ^{228}Ra continuously generate ^{228}Th via radio-decay, while the water mass passed the Korea

Strait reaches to northern parts of the East Sea. ^{228}Th in the polar front area was become closer to secular equilibrium with ^{228}Ra. ^{228}Th/^{228}Ra activity ratios given in table 6 were estimated to be 0.04−0.24 for the surface mixed layer (200 m) in the coastal area (A2) (Table 6; Fig. 10 (a)-(e)).

^{210}Po

Most of ^{210}Po in seawater originate from decay of its parent ^{210}Pb in water column and the atmospheric input. Jung (1995) estimated the ^{210}Pb atmospheric flux into the land and the sea around Korea to be 66 dpm/m^2/d. Assuming the atmospheric flux of ^{210}Po corresponds to about 10% of the atmospheric ^{210}Pb flux (Turekian *et al.*, 1977), we could estimate the atmospheric flux of ^{210}Po to be 6.6 dpm/m^2/d, which is negligible compared to the total ^{210}Po flux of water column. The ^{210}Po vertical flux from euphotic zone was estimated to be in the range of 43−157 dpm/m^2/d at three stations, which were horizontally increased with the distance from the Korea Strait like the case of ^{228}Th flux (Table 3; Fig. 12 (a)). Also, ^{210}Po fluxes in the East Sea were estimated to be 5 times higher than the pelagic flux of 31.5 dpm/m^2/d (Bacon *et al*, 1985), showing vertical increase from 43−157 to 918 dpm/m^2/d with water depth. This trend may be occurred because ^{210}Po constantly produced from their parent nuclide, ^{226}Ra that is almost uniformly distributed in the surface water (Fig. 11 (a)), are cumulatively adsorbed on the surface of sinking particles during their settling and removed in surface water. Therefore, the ^{210}Po vertical flux and its activity in sinking particles were observed to be increased with water depth by the ^{210}Po removal in surface water (Fig. 12 (b)). Because most of the ^{210}Po scavenged by sinking particles exists as labile phase (Bacon *et al.*, 1976), the particulate ^{210}Po are more easily recycled in the process of particle regeneration occurring at shallow sub-surface depths (200 m). Therefore, the recycling processes of particulate phase always make ^{210}Po be in excess relative to ^{226}Ra in water column due to the reflux of regenerated ^{210}Po (Fig. 12 (c)−(e)). Kim and Shin (1997) estimated the ^{210}Po residence time to be 10 years whereas the ^{210}Pb residence time to be 0.5 year in surface water. Because the ^{210}Po residence time is very long compared to its ^{210}Po half-life (138 day), ^{210}Po recycles many times in surface water before removed from the surface water by sinking particles.

CONCLUSION

The ratios of the catched to predicted ^{234}Th flux (F/P ratio) were calculated, assuming that the predicted ^{234}Th flux (P) should be theoretically equal to the catched vertical flux (F) in the overlying water column. Under steady state condition, the theoretical flux (P) could be calculated from the simple relationship $P=P_{^{234}Th}-\lambda C$. The F/P ratios of ^{234}Th were estimated to be 1.0 in surface water, whereas the

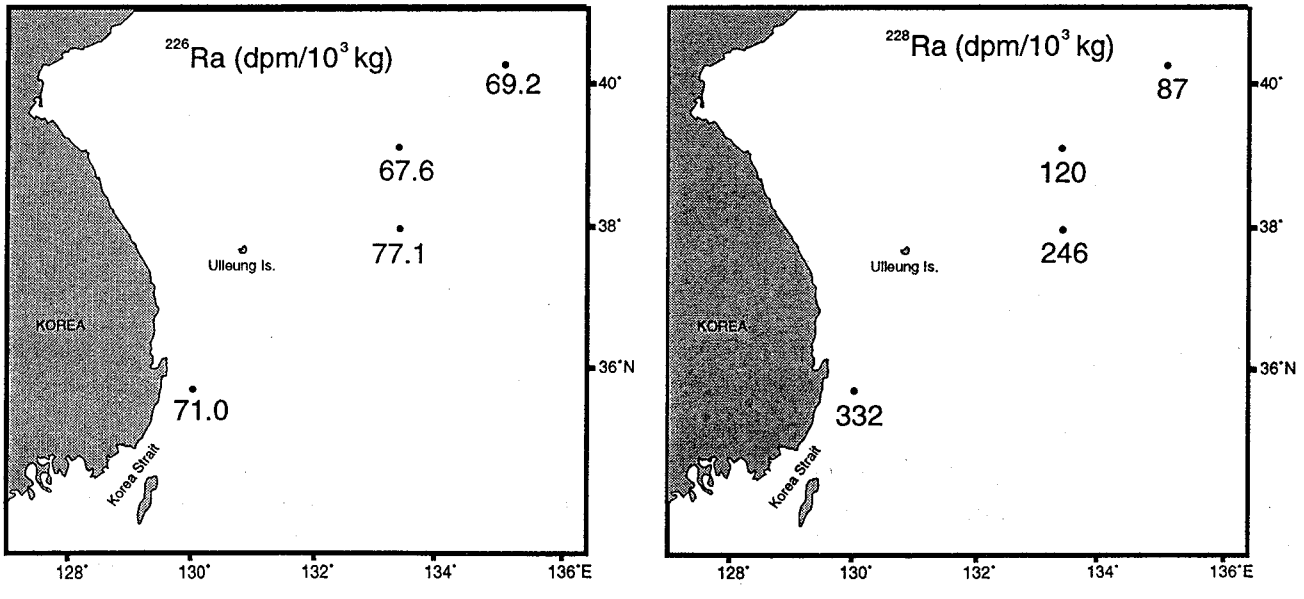

Fig. 11. Horizontal distribution of ^{228}Ra and ^{226}Ra measured at 50 m water depth of the East Sea. ^{228}Ra activities in the surface water gradually decrease from the Korea Strait to polar front, whereas ^{226}Ra homogeneously distribute in this area.

Table 6. The concentrations of total suspended material and activities of ^{234}Th, ^{228}Ra, ^{228}Th, ^{232}Th and ^{210}Po in water column and activities ratios of the daughter to parents nuclides

Station I.D.	Sample Depth (m)	TSM (mg/l)	^{234}Th (dpm/kg)		^{228}Th (dpm/1000 kg)		^{232}Th (dpm/1000 kg)		^{210}Po (dpm/100 kg)	
			Dissolved	Particulate	Dissolved	Particulate	Dissolved	Particulate	Dissolved	Particulate
96-PF-A4	0	0.34	1.36±0.26	0.26±0.02	6.63±0.59	2.47±0.24	0.14±0.05	0.20±0.06	25.40±2.85	15.10±1.42
	50	0.44	1.06±0.22	0.11±0.01	4.44±0.50	2.81±0.22	0.24±0.08	0.50±0.07	30.52±3.09	11.91±1.15
	100	0.31	0.83±0.09	0.49±0.07	3.52±0.31	4.41±0.49	0.21±0.05	0.47±0.14	15.54±0.93	14.45±1.53
	200	0.37	2.06±0.16	0.29±0.02	3.42±0.29	6.94±0.74	0.24±0.05	0.57±0.15	20.49±1.66	12.78±1.15
96-PF-B10	0	0.35	1.25±0.10	0.20±0.02	7.68±0.68	2.70±0.17	4.06±0.39	0.18±0.03	9.99±0.73	3.69±0.27
	50	0.34	1.24±0.29	0.15±0.02	10.40±2.27	7.47±0.46	1.06±0.40	0.32±0.07	4.90±0.35	5.48±0.42
	100	0.35	1.72±0.11	0.18±0.02	3.14±0.21	6.28±0.46	0.94±0.21	1.30±0.16	20.29±1.40	16.32±1.70
	200	0.47	1.99±0.22	0.22±0.02	6.07±0.88	17.82±0.72	0.80±0.20	2.15±0.15	23.50±1.78	12.49±1.05
96-KS-A2	5	10.35	0.41±0.04	1.64±0.07	6.00±0.90	8.40±0.90	4.40±0.80	4.50±0.60	2.94±0.21	8.72±0.60
	50	1.91	1.08±0.06	0.16±0.03	7.20±0.80	3.30±0.50	3.80±0.60	3.60±0.50	2.38±0.14	3.71±0.34
	100	2.52	1.08±0.07	0.13±0.02	7.60±1.00	7.50±0.60	1.30±0.40	1.70±0.30	13.90±0.39	2.63±0.25
	150	1.26	0.96±0.07	0.55±0.04	13.10±1.10	7.00±0.80	3.00±0.50	1.5±0.30	12.85±0.45	2.86±0.18
	200	1.89	1.76±0.10	0.32±0.03	12.30±1.20	5.30±0.50	1.80±0.40	2.10±0.30	17.60±0.51	3.31±0.17
	300	0.88	2.02±0.11	0.51±0.03	65.00±3.60	7.20±0.50	4.40±0.70	1.10±0.20	13.37±0.46	2.43±0.15
	700	1.69	2.00±0.10	0.31±0.03	45.60±2.70	5.80±0.40	2.10±0.50	1.00±0.20	8.82±0.31	2.09±0.12

ratios decreased to under 1.0 in deep sea. This trend was explained by the regeneration of the sinking particles. We could find the evidences for the regeneration of particles in the mass flux profiles and the dissolved and particulate ^{234}Th profiles across thermocline.

The concentrations of the suspended materials at polar front were observed to be constant in water column and showed the similar values at both in the cold and warm water masses in the East Sea (96-PF-A4 and 96-PF-B10), suggesting that the suspended particles play a minor role in transporting particles to the deep sea. The mass fluxes in surface water of warm water mass (1730 mg/m^2/d) were observed to be 3 times greater compared with that in cold water mass (536 mg/m^2/d). Also, the vertical mass fluxes are decreased with increasing water depth. This trend might be generated due to the regeneration of the organic matter in the sinking materials. The available sediment trap data also suggest that the particle mass fluxes are positively correlated with the primary production in euphotic zone. The primary productivity in the warm water mass is observed to be 3 times higher than that in the cold water mass like the case of mass flux. Whereas the suspended materials in the Korea Strait were measured to be higher compared to that of the polar fronts, the vertical mass flux in this region was estimated to be intermediate value between the warm and cold water masses due to the upwelling in this area. We suppose from the decrease of particles flux that 80% of sinking materials are regenerated in warm water mass, where primary productivity is observed to be high in surface water. However, in the cold water mass with little degradable organic matter, the mass fluxes were observed to be uniform in overall water column. It is considered because the organic material regenerable was contained a little in sinking particles of cold water mass by low primary productivity in the surface.

The activities of ^{234}Th, ^{228}Th, ^{232}Th and ^{210}Po in sinking particles were observed to increase with water depth, because Th isotopes hydrated in seawater prefer binding on surface of particles to solution. Because ^{234}Th steadily produced in the water column are cumulatively adsorbed on the surface of sinking particles, vertical ^{234}Th fluxes increased with water depth. Unlike ^{238}U, the ^{228}Ra derived from coastal and shelf sediments disperses over the surface ocean by lateral mixing during its transport toward the polar front. ^{228}Th vertical fluxes increased in proportion to the distance from the Korea Strait, where ^{228}Ra are supplied from terrigenous sediments on continental margins. These facts indicate that the ^{228}Ra diffused out of the sediment in the coastal sea continuously produces ^{228}Th through the radiodecay during transport of the water mass toward polar front. The measured ^{228}Th fluxes were observed to be 4 times higher at the polar front (96-PF-A4 and 96-PF-B10), whereas one-fifth at the Ulleung Basin (96-KS-A2) compared

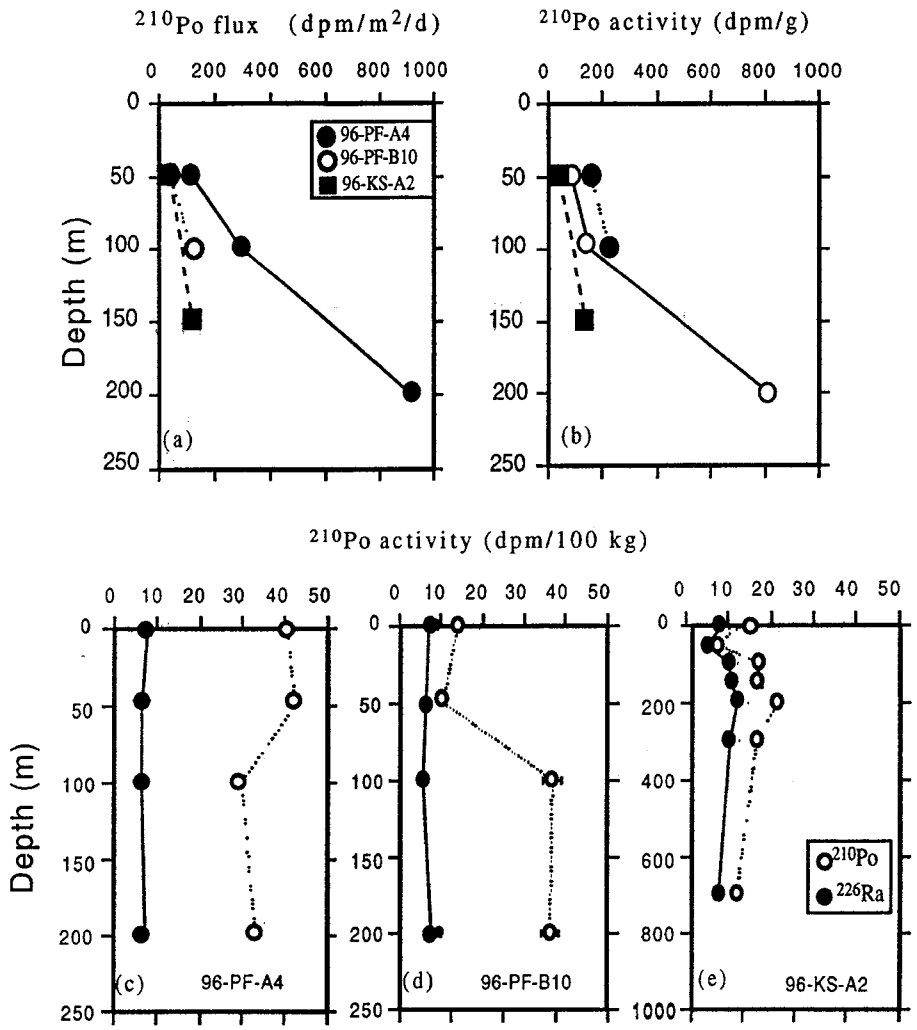

Fig. 12. The vertical fluxes patterns (a) of ^{210}Po according to water depth at three station, 96-PF-A4, 96-PF-B10 and 96-KS-A2, (b) the ^{210}Po specific activity of the sinking particulates and (c) ^{210}Po and ^{226}Ra profiles in water column.

to the predicted fluxes. ^{228}Th in water mass entered into the polar front area are observed to be in secular equilibrium with ^{228}Ra.

Also, this scavenging process produce the radiodisequilibrium between daughter and parent nuclides in water column. The activity ratios of ^{234}Th/^{238}U and ^{228}Th/^{228}Ra were observed to be below 1.0 in the water column above the thermocline and gradually approached to 1.0 in the deep sea. The extent of the deficiency of daughter nuclides compared to their parent nuclides were closely associated with the vertical flux of radionuclides and particles. Because most of the ^{210}Po adsorbed on a labile phase of sinking particles are removed from the euphotic zone and recycled at shallow sub-surface depths (200 m), most of the ^{210}Po collected in the trap of surface water were derived from recycling fraction. Therefore, the ^{210}Po has always come into an excess state relative to ^{226}Ra in surface water column due to the reflux of recycled ^{210}Po.

ACKNOWLEDGEMENT

This study was supported by the grant from the Ministry of Education to K.H.Kim through the Korea Inter-University Institute of Ocean Sciences for the 3-year (1994-1997) project "Oceanographic Characteristic of the Polar Frontal Regions in the East Sea" in which this work was under the second subproject on chemical oceanography.

REFERENCES

Anderson, R.F. and A.P. Fleer, 1982. Determination of natural actinides and plutonium in marine particulate material. *Anal. Chem.*, **54**: 1142–1147.

Anderson, R.F., M.P. Bacon and P.G. Brewer, 1983. Removal of Th-230 and Pa-231 from the open ocean. *Earth Planet. Sci. Letts.*, **62**: 7–23.

Bacon, M.P., C.-A. Huh, A.P. Fleer and W.G. Deuser, 1985. Seasonality in the flux of natural radionuclides and plutonium in the deep Sargasso Sea. *Deep-Sea Res.*, **32**: 273–86.

Bacon, M.P., D.W. Spencer and P.G. Brewer, 1976. $^{210}Pb/^{226}Ra$ and $^{210}Po/^{210}Pb$ disequilibria in seawater and suspended particulate matter. *Earth Planet. Sci. Letts.*, **32**: 277–96.

Baker, E.T., H.B. Milburn and D.A. Tennant, 1988. Field assessment of sediment trap efficiency under varying flow conditions. *J. Mar. Res.*, **46**: 573–592.

Brewer P.G., Y. Nozaki, D.W. Spencer and A.P. Fleer, 1980. Sediment trap experiments in the deep North Atlantic : isotopeic and element fluxes. *J. Mar. Res.*, **38**: 703–728.

Broecker W.S. and T.-H. Peng, 1982. Tracers in the Sea, Eldigio Press, Palisades, New York, 690 pp.

Bruland, K.W., R.P. Franks, W.M. Landing and A. Soutar, 1981. Southern California inner basin sediment trap calibration. *Earth Planet. Sci. Letts.*, **53**: 400–408.

Buesseler K.O., M.P. Bacon, J.K. Cochran, H.D. Livingston, 1992. Carbon and nitrogen export during the JGOFS North Atlantic Bloom Experiment estimated from ^{234}Th : ^{238}U disequilibria. *Deep Sea Res.*, **39**: 1115–1137.

Butman C.A., W.D. Grant and K.D. Stolzenback, 1986. Prediction of sediment trap biases in turbulent flows: a theoretical analysis based on observations from the literature. *J. Mar. Res.*, **44**: 610–644.

Chung Y. and R. Finkel, 1988. ^{210}Po in the Western Indian ocean : distributions, disequilibria and partitioning between the dissolved and particulate phases. *Earth Planet. Sci. Letts.*, **88**: 232–240.

Clegg S. L. and M. Whitfield, 1990. A generalized model for the scavenging of trace metals in the opening ocean. II-Thorium scavenging. *Deep-Sea Res.*, **38**: 91–120.

Clegg S. L. and M. Whitfield, 1993. Application of a generalized scavenging model to time series ^{234}Th and particle data obtained during the JGOFS North Atlantic Bloom Experiment. *Deep-Sea Res.*, **40**: 1529–1545.

Coale, K.H. and K.W. Bruland, 1985. Th-234/U-238 disequilibria within the California Current. *Limnol. Oceanogr.*, **30**: 22–33.

Cochran J.K., K.O. Buesseler, M.P.Bacon and H.D. Livingston, 1993. Thorium isotopes as indicators of particle dynamics in the upper ocean : results from the JGOFS North Atlantic Bloom Experiment. *Deep-Sea Res.*, **40**: 1569–1595.

Deuser, W.G., E.H. Ross and R.F. Anderson, 1981. Seasonality in the supply of sediment to the deep Sargasso Sea and implications for the rapid transport of matter to the deep ocean. *Deep-Sea Res.*, **28**: 495–505.

Deuser, W.G. and E.H. Ross, 1980. Seasonal change in the flux of organic carbon to the deep Sargasso sea. *Nature*, **283**: 364–365.

Dymond, J., K. Fischer, M. Clauson, R. Cobler, W. Gardner, M. J. Richardson, W. Berger, A Soutar, and R. Dunbar, 1981. A sediment trap intercomparison study in the Santa Barbara Basin. *Earth Planet. Sci. Letts.*, **53**: 409–418.

Fleer A.P. and M.P. Bacon, 1984. Determination of lead-210 and polonium-210 in seawater and marine particulate matter. Neclear Instruments and Methods in Physics Research, **223**: 234–249.

Gamo T. and Y. Horibe, 1983. Abyssal circulation in the Japan sea. *J. Oceanogr. Soc. Jpn.*, **39**: 220–230.

Gardner W.D., 1980. Field assessment of sediment traps. *J. Mar. Res.*, **38**: 41–52.

Harada K. and Tsunogai S., 1985. A particle method for the simultaneous determinations of ^{234}Th, ^{226}Ra, ^{210}Pb and ^{210}Po in seawater. *J. Oceanogr. Soc. Jpn.*, **41**: 98–104.

Harada K. and Tsunogai S., 1986. ^{226}Ra in the Japan Sea and the residence time of the Japan sea water. *Earth Planet. Sci. Letts.*, **77**: 236–244.

Hata K., 1962. Seasonal variation of the volume transport in the northern part of the Japan sea. *J. Oceanogr. Soc. Jpn.* 20th Anniversary Volume, pp. 168–179.

Huh C.A. and Beasley T., 1987. Profiles of dissolved and particulate thorium isotopes in the water column of coastal Southern California. *Earth Planet. Sci. Letts.*, **85**: 1–10.

Huh C.A, T.L. Ku, S. Luo, M.R.Landry and P.M.willians, 1993. Fluxes of Th isotopes in the Santa Monica Basin, offshore California. *Earth Planet Sci. Letts.*, **116**: 155–164.

Jickells, T.D., W.G. Deuser and A.H. Knap, 1984. The sedimentation rates of trace elements in the Sargasso Sea measured by sediment trap. *Deep-Sea Res.*, **31**: 1169–1178.

Jung, H.S., 1995. Estimation of Atmospheric Fluxes of Cosmogenic Radionuclides ^{7}Be and ^{210}Pb and Anthropogenic Metals, Master's thesis, Chungnam National University, Taejon, Korea, 52 pp.

Kaufman, A., Y.-H. Li and K. K. Turekian, 1981. The removal rates of ^{234}Th and ^{228}Th from waters of the New York Bight. *Earth Planet. Sci. Letts.*, **54**: 385–392.

Kim C.H. and Kim K, 1983. Characteristics and origin of the cold water mass along the East coast of Korea. *J. Oceanogra. Soc. Kor.*, **18**: 78–83.

Kim K.H and H.-B Shin, 1997. Scavenging of ^{210}Pb and ^{210}Po in the coastal waters of the southern East Sea. *Radioprotection, Colloques*, **32**: 23–28.

KIOS, 1996. Oceanographic Characteristics of the polar frontal regions in the East Sea, pp. 116–156.

Knauer, G. A., J. H. Martin and K. W. Bruland, 1979. Fluxes of particulate carbon, nitrogen, and phosphorus in the upper water column of the north east Pacific. *Deep-Sea Res.*, **26**: 97–108.

Li Y.H., H.W. Feely and J.R. Toggweiler, 1980. ^{228}Ra and ^{228}Th concentration in GEOSECS Atlantic surface water. *Deep-Sea Res.*, **27**: 545–555.

McCave, 1975. Vertical flux of particles in the ocean. *Deep-sea Res.*, **22**: 491–502.

McKee B.A., DeMaster D.J., Nittrouer C.A., 1984. The use of $^{234}Th/^{238}U$ disequilibrium to examine the fate of particle-reactive species on the Yangtz continental shelf. *Earth Planet. Sci. Letts.*, **68**: 431–442.

Moore, W. S., K. W. Bruland and J. Michel, 1981. Fluxes of uranium and thorium series isotopes in the Santa Barbara Basin. *Earth Planet. Sci. Letts.*, **53**: 391–399.

Moriyasu S., 1972. The Tsushima current, In : Kuroshio; its physical aspects. H. Stommel and K. Yoshida, editors, University of Tokyo press, Tokyo, pp. 353–369

Nitani, 1972. On the deep and bottom waters in the Japan sea. In: Research in Hydrography and the Oceanography, edited by D. Shoji, editor, Hydrographic Department of Japan, Tokyo, pp. 151–201.

Noh Il, 1988. Algal pigments and their degradation products in southern ocean and Gulf of Mexico surface waters. Dissertation thesis, Texas A&M University, 143 pp.

Nozaki Y. and M.Yamada, 1987. Thorium and protactinium isotope distributions in waters of the Japan sea. *Deep-Sea Res.*, **34**: 1417–1430.

Nozaki, Y., H.-S. Yang and M. Yamada, 1987. Scavenging of thorium in the ocean. *J. Geophys. Res.*, **92**: 772–778.

Shim J.H. and Y.C. Park, 1984. Community structure and spatial distribution of phytoplankton in the southwestern sea of Korea, in early summer. *J. Oceanogr. Soc. Korea*, **19**: 68–81.

Suess, E., 1980. Particulate organic carbon flux in the ocean—surface productivity and oxygen utilization. *Nature*, **288**: 260–263.

Suzuki, 1994. Relationship between atmospheric fluxes and concentrations of terrigenous materials in the surface air over the Japan sea. *J.Oceanogra.*, **50**: 173–178.

Tsunogai S., M. Kawasaki, K. Harada, 1994. Different partitioning among Thorium isotopes in seawater of the Northern North Pacific. *J. Oceanogra.*, **50**: 197–207.

Uda M., 1934. Hydrographical studies based on simultaneous oceanographic surveys made in the Japan sea and its adjacent waters during May and June, 1932. Record of Oceanographic works in japan. **6**: 19–107.

Wei C.L.and J.W. Murray, 1992. Temporal variations of ^{234}Th activity in the water column of Dabob Bay : Particle scavenging. *Limnol. Oceanogr.*, **34**: 296–314.

Yoon, J.H., 1982. Numerical experiment on the circulation in the Japan sea. Part II. Influence of seasonal variations in atmospheric conditions in the Tsushima current. *J. Oceanogra. Soc. Jpn.*, **38**: 81–94.

Manuscript received April 16, 1998
Revision accepted November 24, 1999